RESEARCH ARTICLE | JANUARY 17 2025

Enhanced quantum synchronization of a driven qubit under structured reservoir

Po-Wen Chen ✉; Chandrashekar Radhakrishnan; Md Manirul Ali

APL Quantum 2, 016109 (2025)
https://doi.org/10.1063/5.0242574

Enhanced quantum synchronization of a driven qubit under structured reservoir

Cite as: APL Quantum 2, 016109 (2025); doi: 10.1063/5.0242574
Submitted: 5 October 2024 • Accepted: 30 December 2024 •
Published Online: 17 January 2025

Po-Wen Chen,[1,a)] Chandrashekar Radhakrishnan,[2,b)] and Md Manirul Ali[3,c)]

AFFILIATIONS

[1] Department of Physics, National Atomic Research Institute, Taoyuan City 325207, Taiwan
[2] Department of Computer Science and Engineering, New York University Shanghai, 567 West Yangsi Road, Pudong, Shanghai 200124, China
[3] Centre for Quantum Science and Technology, Chennai Institute of Technology, Chennai 600069, India

[a)] **Author to whom correspondence should be addressed:** powen@nari.org.tw
[b)] chandrashekar.radhakrishnan@nyu.edu
[c)] manirul@citchennai.net

ABSTRACT

Synchronizing a few-level quantum system is of fundamental importance to the understanding of synchronization in the deep quantum regime. We investigate quantum phase synchronization of a two-level system (qubit) driven by a semiclassical laser field, in the presence of a dissipative environment having finite bath correlation. The phase preference of the qubit is demonstrated through the Husimi Q-function, and the existence of a limit cycle is also shown in our system. Synchronization of the qubit is quantified using the shifted phase distribution. The signature of quantum phase synchronization viz. the Arnold tongue is obtained from the maximal value of the shifted phase distribution. Two distinct types of qubit dynamics are considered depending on the reservoir correlation time being very short and a situation when bath correlation time is finite. When the reservoir's frequency spectrum is broad and the bath correlation time is short, the qubit's phase preference vanishes in the long-time limit. In contrast, a finite bath correlation time and narrow spectral density result in persistent long-time phase localization. The synchronization regions are governed by system–environment parameters, with qubit phase synchronization being enhanced when the reservoir exhibits a narrow frequency spectrum.

I. INTRODUCTION

Synchronization is a natural phenomenon that occurs in a variety of physical, chemical, and biological systems and has been extensively studied and observed in nature for many years.[1–6] For example, if an autonomous oscillating system is coupled to another such system or an external driving force, it can synchronize its frequency and phase to the external system/driving.[7] A well-known example of classical synchronization is the van der Pol oscillator model.[4–6] In recent past, the van der Pol oscillator model was reformulated in terms of a quantum system,[8–11] and it was shown that when the system is far from the ground state, synchronization in quantum systems is analogous to classical synchronization under the influence of noise.[8] When we are close to the ground state, this correspondence is changed because the discreteness of the energy levels becomes important. It is, therefore, interesting to study synchronization in quantum systems with a small number of energy levels. Studying synchronization of finite dimensional quantum systems have gained momentum due to its potential application in the field of quantum computation and quantum information. Recently, quantum synchronization in low-dimensional systems has been investigated.[12–16] Generally synchronization can be classified into forced synchronization and spontaneous synchronization (or mutual synchronization). In the case of spontaneous synchronization,[17–25] the interested system becomes synchronized in the transient evolution of dynamical systems due to the interaction between the subsystems or an external environment. In contrast to spontaneous synchronization, forced synchronization or entrainment usually emerges with externally driven forces.[9,12–16,26] Here, we investigate the quantum phase synchronization of a two-level system in the presence of an external driving field. Synchronizing a few-level quantum system is of fundamental importance to the understanding of synchronization in the deep quantum regime. Initially in Refs. 12, 19, 20, and 26, qubits

were suggested to be the smallest possible system that can be synchronized. Later, spin-1 systems were theoretically shown to be synchronizable,[13,14,22] experimental demonstrations of which were carried out subsequently.[27,28] However, in Ref. 13, it was claimed that quantum synchronization is not applicable for a single qubit (spin-1/2 system) due to the lack of limit cycle. Subsequently, it was shown that the limit cycle of a single qubit can be obtained and synchronization of a qubit to an external signal is possible.[15,16] Following that, synchronization of a single qubit to an external driving signal is experimentally demonstrated using a trapped-ion system.[29]

In the present work, we investigate quantum phase synchronization for a two-level system (qubit) driven by a semiclassical laser field and simultaneously coupled to a dissipative environment; existence of the limit cycle is shown in our system. We analyze the phase synchronization of a driven qubit under two distinct scenarios: (i) a reservoir with a broad frequency spectrum and negligible memory, and (ii) a reservoir with a narrow spectral density and finite bath correlation time. In our analysis, we have considered an Ohmic spectral density that simulates the two-level open quantum system. However, our synchronization analysis for the two-level system is applicable to any other structured reservoir as well. For example, one can also consider sub-Ohmic, super-Ohmic, or a more general spectral density. Recently, non-Markovian environments have drawn particular attention in quantum science and technology when environment's correlation time is not too small compared to the system's relaxation time in many physical systems.[30,31] It is interesting to investigate the relationship between non-Markovianity and quantum synchronization.[16,32–34] Here, we show that the reservoir memory has a significantly positive impact on the emergence of quantum phase synchronization. The rest of the paper is organized as follows: in Sec. II, we consider a widely studied two-level system (qubit) simultaneously interacting with a dissipative environment while being driven by an external field. The time evolution of the reduced density matrix of the qubit is considered to be two distinct types of dynamics, depending on (1) the reservoir correlation time is very small compared to the qubit's relaxation time and the dynamics is defined as Markovian dynamics and (2) the reservoir correlation time is of the same order as the system relaxation time and connected with non-Markovian memory effects.[35–43]

In Sec. III, we demonstrate the transient dynamics of the Husimi Q-representation in order to visualize and characterize phase synchronization behavior in both the Markov and non-Markov regimes. In Sec. IV, we consider a measure of synchronization, called shifted phase distribution, and show its dynamics as a function of phase and detuning in the Markovian and non-Markovian regimes. We also plot the maximum value of the shifted phase distribution in two different ways: (a) by varying the detuning and laser drive strength and (b) by varying the system–bath coupling and laser drive strength. Signature of quantum phase synchronization viz. the Arnold tongue is demonstrated through the maximal value of the shifted phase distribution. Finally, we present our conclusions in Sec. V.

II. MODEL OF LASER-DRIVEN QUBIT AND TIME EVOLUTION

A single two-level system (TLS) driven by a semiclassical laser field is coupled to a dissipative environment. In this study, we work with the rotating wave approximation (RWA) and the total Hamiltonian of the system plus environment and the external driving is given by

$$H = H_S + H_R + H_{SR} + H_d = \frac{\hbar}{2}\omega_0\sigma_z + \sum_k \hbar\omega_k b_k^\dagger b_k + \sum_k \hbar\left(g_k\sigma_+ b_k + g_k^*\sigma_- b_k^\dagger\right) + i\hbar\frac{\epsilon}{4}\left(e^{i\omega_L t}\sigma_- + e^{-i\omega_L t}\sigma_+\right), \quad (1)$$

where the ground state to excited state transition frequency is ω_0. The strength of the semi-classical laser field is ϵ and its driving frequency is ω_L. The system Hamiltonian H_S can be written in terms of the spin-raising and spin-lowering operators $\sigma_+ = |1\rangle\langle 0|$ and $\sigma_- = |0\rangle\langle 1|$. The Hamiltonian of the dissipative environment H_R is described by a collection of infinite bosonic modes with the bosonic creation and annihilation operators denoted by $b_k^\dagger$ and b_k, respectively. The factor g_k is the coupling strength between the system and the kth mode of the environment with frequency ω_k. Using the unitary transformation, $U(t) = e^{\frac{i}{2}\sigma_z\omega_L t}$, we transform the Hamiltonian to a frame rotating at the laser driving frequency. The total Hamiltonian after this transformation reads

$$H = H_{\rm TLS} + H_{\rm SR} + H_{\rm R} = \frac{\hbar}{2}\Delta\sigma_z + \frac{\hbar}{2}\epsilon\sigma_x + \sum_k \hbar\left(g_k\sigma_+ b_k e^{i\omega_L t} + g_k^*\sigma_- b_k^\dagger e^{-i\omega_L t}\right) + \sum_k \hbar\omega_k b_k^\dagger b_k, \quad (2)$$

where $\Delta = \omega_0 - \omega_L$ represents the detuning with the laser driving. The two-level system Hamiltonian can precisely be diagonalized as

$$H_{\rm TLS} = \frac{\hbar}{2}\Delta\sigma_z + \frac{\hbar}{2}\epsilon\sigma_x = \frac{\hbar}{2}\delta\tilde{\sigma}_z, \quad (3)$$

where we use the basis transformation $|\tilde{1}\rangle = \cos\frac{\theta}{2}|1\rangle + \sin\frac{\theta}{2}|0\rangle$ and $|\tilde{0}\rangle = -\sin\frac{\theta}{2}|1\rangle + \cos\frac{\theta}{2}|0\rangle$, and we choose $\tan\theta = \frac{\epsilon}{\Delta}$ and $\delta = \sqrt{\Delta^2 + \epsilon^2}$. In the new basis, the spin operators are defined as $\tilde{\sigma}_+ = |\tilde{1}\rangle\langle\tilde{0}|$, $\tilde{\sigma}_- = |\tilde{0}\rangle\langle\tilde{1}|$, and $\tilde{\sigma}_z = |\tilde{1}\rangle\langle\tilde{1}| - |\tilde{0}\rangle\langle\tilde{0}|$. The system–reservoir interaction Hamiltonian in the interaction picture reads

$$H_{\rm SR}(t) = \sum_k \hbar g_k[\alpha\tilde{\sigma}_z + \eta\tilde{\sigma}_+ + \mu\tilde{\sigma}_-]b_k\, e^{i(\omega_L-\omega_k)t} + \text{H.c.}, \quad (4)$$

where $\alpha = \frac{\epsilon}{2\delta}$, $\eta = \frac{\Delta+\delta}{2\delta}$, and $\mu = \frac{\Delta-\delta}{2\delta}$. The interaction Hamiltonian can finally be expressed as

$$H_{\rm SR}(t) = S(t)B(t) + \text{H.c.}, \quad (5)$$

where the reservoir operator $B(t)$ and the factor $S(t)$ are defined as

$$B(t) = \sum_k g_k b_k e^{-i\omega_k t};\ S(t) = \left(\alpha\tilde{\sigma}_z + \eta\tilde{\sigma}_+ e^{i\delta t} + \mu\tilde{\sigma}_- e^{-i\delta t}\right)e^{i\omega_L t}. \quad (6)$$

The constant α denotes the elastic tunneling through the bath, whereas the η and μ denotes the inelastic excitation and relaxation through the bath, respectively. For simplicity, we consider the factorized initial system–environment state $\rho_T(0) = \rho(0)\otimes\rho_E(0)$, where $\rho(0)$ is the initial state of the system and the reservoir is initially in a thermal equilibrium state $\rho_E(0)$, given by

$$\rho_E(0) = \exp(-\beta H_{\rm R})/{\rm Tr}[\exp(-\beta H_{\rm R})]. \quad (7)$$

Here, $\beta = 1/k_B T$ with k_B is the Boltzmann constant and T is the temperature. We have adopted a general framework to derive a perturbative quantum master equation, and for simplicity, we consider a zero-temperature reservoir here. The second-order perturbative master equation in the Schrödinger picture for the two-level system is then given by

$$\begin{aligned}\frac{d\rho}{dt} = &-\frac{i\delta}{2}[\sigma_z, \rho] + \big[\Gamma_1(t)\{\alpha^2(\sigma_z\rho\sigma_z - \sigma_z\sigma_z\rho) \\ &+ \alpha\eta(\sigma_z\rho\sigma_+ - \sigma_+\sigma_z\rho) + \alpha\mu(\sigma_z\rho\sigma_- - \sigma_-\sigma_z\rho)\} \\ &+ \Gamma_2(t)\{\mu\alpha(\sigma_+\rho\sigma_z - \sigma_z\sigma_+\rho) + \mu\eta(\sigma_+\rho\sigma_+ - \sigma_+\sigma_+\rho) \\ &+ \mu^2(\sigma_+\rho\sigma_- - \sigma_-\sigma_+\rho)\} + \Gamma_3(t)\{\eta\alpha(\sigma_-\rho\sigma_z - \sigma_z\sigma_-\rho) \\ &+ \eta^2(\sigma_-\rho\sigma_+ - \sigma_+\sigma_-\rho) + \eta\mu(\sigma_-\rho\sigma_- - \sigma_-\sigma_-\rho)\} + \text{H.c.}\big], \quad (8)\end{aligned}$$

where we have omitted the bars from the spin operators and it is implicit that the Pauli spin operators are now in the new basis. The time dependent coefficients in the master equation are denoted by

$$\Gamma_1(t) = \int_0^t d\tau \int_0^\infty d\omega J(\omega) e^{-i(\omega-\omega_L)(t-\tau)}, \quad (9)$$

$$\Gamma_2(t) = \int_0^t d\tau \int_0^\infty d\omega J(\omega) e^{-i(\omega-\omega_L+\delta)(t-\tau)}, \quad (10)$$

$$\Gamma_3(t) = \int_0^t d\tau \int_0^\infty d\omega J(\omega) e^{-i(\omega-\omega_L-\delta)(t-\tau)}. \quad (11)$$

The master equation (8) is a convolution-less time-local differential equation. The time-dependent coefficients $\Gamma_1(t)$, $\Gamma_2(t)$, and $\Gamma_3(t)$ account for the memory effect of the non-Markovian environment. To characterize the environment and calculate these time-dependent coefficients in Eqs. (9)–(11), we must consider a spectral density to characterize the structured environment. The time-dependent correlation functions fully characterize the non-Markovian memory effect given the spectral density $J(\omega)$. Here, we consider an Ohmic spectral density,[36,40,44–46] which is a common class of spectral density that simulates the dynamics of a two-level open quantum system,

$$J(\omega) = \gamma\omega \exp(-\omega/\lambda). \quad (12)$$

Our formalism is applicable to any spectral distribution, making the phase synchronization analysis for the two-level system suitable for more general structured reservoirs. The time-dependent coefficients (9)–(11) appearing in the master equation contain the non-Markovian characteristics of the open quantum system. Here, γ is the coupling strength between the system and dissipative bath and is measured in units of γ_0, which is a fixed frequency, closely related to the relaxation time of the qubit. The constant γ_0 is the relaxation rate related to the T_1 relaxation time of the qubit under spontaneous decay. Considering a typical experimental value of the relaxation time of a superconducting qubit,[47–49] we find the relaxation rate γ_0 to be of the order of MHz. In this work, we have taken $\gamma = 0.1\gamma_0$ for all results where coupling strength γ is fixed. The parameter λ is the cutoff frequency of the bath spectrum. We see two distinct types of qubit dynamics based on the value of the system–environment parameters. For $\lambda > 2\gamma$, the reservoir correlation time is very short compared to the relaxation time of the qubit and, consequently, the dynamics is Markovian. When $\lambda < 2\gamma$, the reservoir correlation time is comparable with the relaxation time of the qubit, and hence, we observe non-Markovian memory effects. For the Markov regime, we consider a value of $\lambda = 5\gamma_0$, and in the non-Markov regime, $\lambda = 0.01\gamma_0$. We investigate the phase synchronization of the driven qubit with a finite detuning $\Delta = \gamma_0$.

Next, we investigate the features of synchronization of a driven two-level system using the Husimi Q-function. The Husimi Q-function is one of the simplest distributions of quasiprobability in phase space.[50] We show a robust, long-time synchronous dynamics of the qubit under a non-Markovian structured environment. The phase preference or dynamical phase localization of the qubit is observed and quantified through an investigation of the Husimi Q-function.[13–15,22] The phase distribution function and the shifted phase distribution (see Secs. IV A and IV B) obtained from the Husimi Q-function indicate the presence of a dynamical phase localization. This dynamical phase localization can also be quantified by the maximum value of the shifted phase distribution. From the characterization of the maximum value of the shifted phase distribution, we observe the formation of a triangular region which demarcates the space into regions where phases are either localized or delocalized. This feature is well-known in the theory of synchronization as Arnold tongue.

III. HUSIMI Q-FUNCTION

The phase synchronization of the driven TLS can be characterized using the Husimi Q-function,[50,51] which is a quasi-probability distribution capable of capturing the phase space dynamics. In our work ,we use the spin-coherent states and the corresponding expression reads

$$Q(\theta, \phi, t) = \frac{1}{2\pi}\langle\theta, \phi|\rho(t)|\theta, \phi\rangle, \quad (13)$$

where $\rho(t)$ is the time-evolved density matrix. For the two-level system, $|\theta, \phi\rangle$ are the spin-coherent states, which are eigenstates of the spin operator $\sigma_n = \hat{\mathbf{n}} \cdot \hat{\sigma}$ along the unit vector $\hat{\mathbf{n}}$ with polar coordinates θ and ϕ. This state $|\theta, \phi\rangle = \cos(\theta/2)|1\rangle + \sin(\theta/2)e^{i\phi}|0\rangle$ represents a point on the surface of a Bloch sphere, where $|0\rangle$ and $|1\rangle$ are the eigenstates of the spin operator σ_z. Once the temporal evolution of reduced density matrix is determined from Eq. (8), it is easy to obtain the time dynamics of Q-distribution as a function θ, ϕ, and t as follows:

$$\begin{aligned}Q(\theta, \phi, t) = &\frac{1}{2\pi}\text{Tr}(|\theta, \phi\rangle\langle\theta, \phi|\rho(t)) = \frac{1}{2\pi}\text{Tr} \\ &\times\left[\begin{pmatrix}\cos^2(\theta/2) & \sin(\theta/2)\cos(\theta/2)e^{-i\phi} \\ \sin(\theta/2)\cos(\theta/2)e^{i\phi} & \sin^2(\theta/2)\end{pmatrix}\right. \\ &\left.\times\begin{pmatrix}\rho_{11}(t) & \rho_{10}(t) \\ \rho_{01}(t) & \rho_{00}(t)\end{pmatrix}\right], \\ = &\frac{1}{2\pi}\big[\cos^2(\theta/2)\rho_{11}(t) + \sin(\theta/2)\cos(\theta/2)e^{-i\phi}\rho_{01}(t) \\ &+ \sin(\theta/2)\cos(\theta/2)e^{i\phi}\rho_{10}(t) + \sin^2(\theta/2)\rho_{00}(t)\big]. \quad (14)\end{aligned}$$

From Eq. (14), we can see that the Q-function can be expressed as a weighted sum of the individual density matrix elements. An

analysis of the time-evolved Q-function for the Markovian and non-Markovian evolution is shown in Fig. 1 for an initial state of $|+\rangle = (|0\rangle + |1\rangle)/\sqrt{2}$. In Fig. 1(a), the Husimi Q-function for the Markov dynamics is shown in the long-time limit of $\gamma t = 500$. At time $t = 0$, we observed that the Q-function is nonuniformly distributed and it is peaked at $\phi = 0$. As the system evolves in time, the phase distribution becomes more and more uniform, and in the long-time limit, the phase preference is diminished under Markov evolution when the reservoir's frequency spectrum is broad and the bath correlation time is short. We have taken $\lambda = 5\gamma_0$, $\Delta = \gamma_0$, and $\epsilon = \gamma_0$ for this Markov evolution. In Fig. 1(b), we show the Q-function of the driven qubit in the non-Markovian regime ($\lambda = 0.01\gamma_0$). The detuning is fixed at $\Delta = \gamma_0$, driving amplitude $\epsilon = \gamma_0$, and the evolution time is taken as $\gamma t = 500$. In contrast to the Markov case, we find here that the phase delocalization process is significantly slowed down under non-Markov dynamics when the bath correlation time is extended for a narrow spectral density of the reservoir. This leads to a non-uniform phase distribution, indicating the presence of phase preference in the system, where the phase remains localized rather than spread out. Under this non-Markovian evolution, only the relative position of the Q-function peak shifts at around $\phi = \pi/2$. The system–environment coupling strength is taken as $\gamma = 0.1\gamma_0$ for all the plots shown in Fig. 1. Hence, we can conclude that the phase localization is enhanced under non-Markovian evolution if we compare the dynamics to its Markovian counterpart.

The relative phase in a quantum system is encoded in the off-diagonal elements. Hence, any phase localization will imply that the off-diagonal elements survive in the long time limit. In Fig. 2, we show the evolution of $|\rho_{10}(t)|$ for both Markovian and non-Markovian dynamics, with varying driving amplitude ϵ. For Markovian evolution ($\lambda = 5\gamma_0$), the value of $|\rho_{10}(t)|$ decays very fast when the driving amplitude ϵ is very small. In this case, we do not see quantum phase localization in the long time. The magnitude of $|\rho_{10}(t)|$ saturates to a finite value in the long time limit as we increase the driving amplitude ϵ. Under Markov dynamics ($\lambda = 5\gamma_0$), the phase localization is not completely wiped out in the presence of the driving field. This is what we see from the plot of Husimi Q-function in Fig. 1(a). The long-time saturation value of $|\rho_{10}(t)|$ crucially depends on the value of ϵ. In the case of non-Markovian evolution,

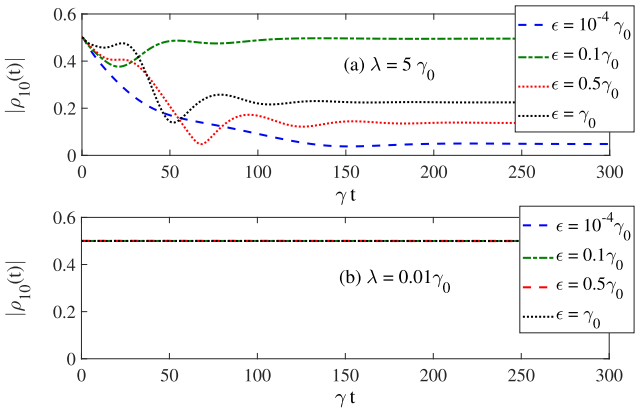

FIG. 2. Plot of the magnitude of off-diagonal element $|\rho_{10}(t)|$ as a function of time is given for (a) Markov dynamics when the bath correlation time is short and (b) non-Markovian evolution when the bath correlation time is extended for a narrow spectral density of the reservoir. The system–environment coupling strength is taken as $\gamma = 0.1\gamma_0$.

the value of the off-diagonal element $|\rho_{10}(t)|$ remains almost constant throughout the evolution and is the same for different values of the driving amplitude ϵ. In the presence of non-Markovian memory effect, the driven qubit exhibits quantum phase localization when the structured reservoir has a narrow spectral density and a finite bath correlation time.

It is well-known that the off-diagonal elements signal the presence of quantum coherence in the system. Hence, we conclude that the quantum phase localization and, consequently, the quantum phase synchronization is due to long lasting quantum coherence in the system. This relationship between quantum phase synchronization and quantum coherence has been examined in detail in Ref. 43. The synchronization in our work is quite different from the ones discussed in Refs. 24 and 33. In these references, there are two coupled quantum systems of which one is connected to an external bath and they study the synchronization of the systems in the absence of the driving field and this type of synchronization is referred to as spontaneous mutual synchronization.

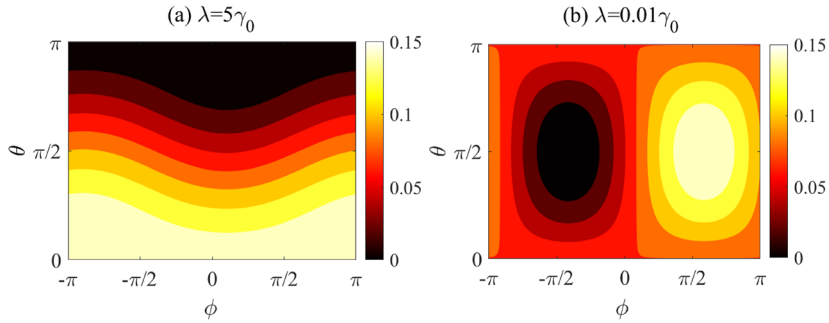

FIG. 1. Husimi Q-function of a single qubit coupled to a dissipative bath in the presence of an external driving is shown under (a) Markovian dynamics when the reservoir memory is negligible and (b) non-Markovian dynamics with narrow spectral density. We have taken the spectral width $\lambda = 5\gamma_0$ for Markovian evolution and $\lambda = 0.01\gamma_0$ for non-Markovian evolution. The values of the other parameters are taken as $\Delta = \gamma_0$, $\epsilon = \gamma_0$, $\gamma = 0.1\gamma_0$, and $\gamma t = 500$.

IV. SYNCHRONIZATION MEASURE AND ARNOLD'S TONGUE

A. Shifted phase distribution

The Husimi Q-function can be used to identify the phase preference in the two-level quantum system. To find the strength of the phase preference, we adopt the measure proposed in Refs. 13–15. This function is obtained by integrating the Q-function over the angular variable "θ" to get the phase distribution $P(\phi,\rho) = \int Q(\theta,\phi,t)\sin\theta d\theta$ for a given state ρ. A quantum state with uniform phase distribution has $P(\phi,\rho_0) = 1/2\pi$. So, the non-uniformity in the phase distribution or rather the phase preference can be measured using a function called the shifted phase distribution given in the following:

$$S(\phi,t) \equiv P(\phi,\rho) - P(\phi,\rho_0) = \int_0^\pi Q(\theta,\phi,t)\sin\theta d\theta - \frac{1}{2\pi}. \quad (15)$$

This function is zero if there is no phase localization, which implies there will not be any phase synchronization. We substitute $Q(\theta,\phi,t)$ from Eq. (14) in Eq. (15) to evaluate the integral over the angular variable θ as follows:

$$\begin{aligned} S(\phi,t) = -\frac{1}{2\pi} + \frac{1}{2\pi}\Big[&\rho_{11}(t)\int_0^\pi \cos^2(\theta/2)\sin\theta d\theta \\ &+ \rho_{00}(t)\int_0^\pi \sin^2(\theta/2)\sin\theta d\theta \\ &+ \rho_{10}(t)\, e^{i\phi}\int_0^\pi \sin(\theta/2)\cos(\theta/2)\sin\theta d\theta \\ &+ \rho_{01}(t)\, e^{-i\phi}\int_0^\pi \sin(\theta/2)\cos(\theta/2)\sin\theta d\theta\Big]. \end{aligned} \quad (16)$$

Evaluating the integral over the angular variable θ in Eq. (16) and using the condition of trace invariance i.e., $\rho_{00}(t) + \rho_{11}(t) = 1$, we get

$$S(\phi,t) = \frac{1}{8}\Big[\rho_{10}(t)e^{i\phi} + \rho_{01}(t)e^{-i\phi}\Big]. \quad (17)$$

We plot the shifted phase distribution $S(\phi,t)$ as a function of Δ and ϕ at different instants of time in both the Markovian and non-Markovian regime. In Fig. 3(a), we plot $S(\phi,t)$ under Markovian dynamics with a wide spectrum ($\lambda = 5\gamma_0$) in which subplots Figs. 3(a1) and 3(a2) describe the variation of $S(\phi,t)$ with Δ and ϕ for $\gamma_0 t = 10$ and $\gamma_0 t = 500$, respectively. From Fig. 3(a1), we find that there are V-shaped yellow regions of phase localization in the short-time $\gamma_0 t = 10$. With the increase in $\gamma_0 t$, we observe that the regions with $S(\phi,t) = 0$ increases and for $\gamma_0 t = 500$, the shifted phase distribution becomes almost uniform over ϕ, as shown in Fig. 3(a2). The non-Markovian dynamics with narrow spectrum ($\lambda = 0.01\gamma_0$) of the shifted phase distribution $S(\phi,t)$ is shown in Fig. 3(b). Subplots Figs. 3(b1) and 3(b2) demonstrate $S(\phi,t)$ as a function of Δ and ϕ for evolution time $\gamma_0 t = 10$ and $\gamma_0 t = 500$, respectively. Here, we again show phase localization regions in Fig. 3(b1) for $\gamma_0 t = 10$. While the characteristics of this region change with time, the shifted phase distribution never becomes zero uniformly for all values of Δ and ϕ even when $\gamma_0 t = 500$, as shown in Fig. 3(b2). There are periodic finite values of Δ where the phase synchronization occurs. Hence, our results show that the phase localization disappears in the long-time limit for Markovian dynamics with negligible reservoir memory. In the case of non-Markovian dynamics, the phase

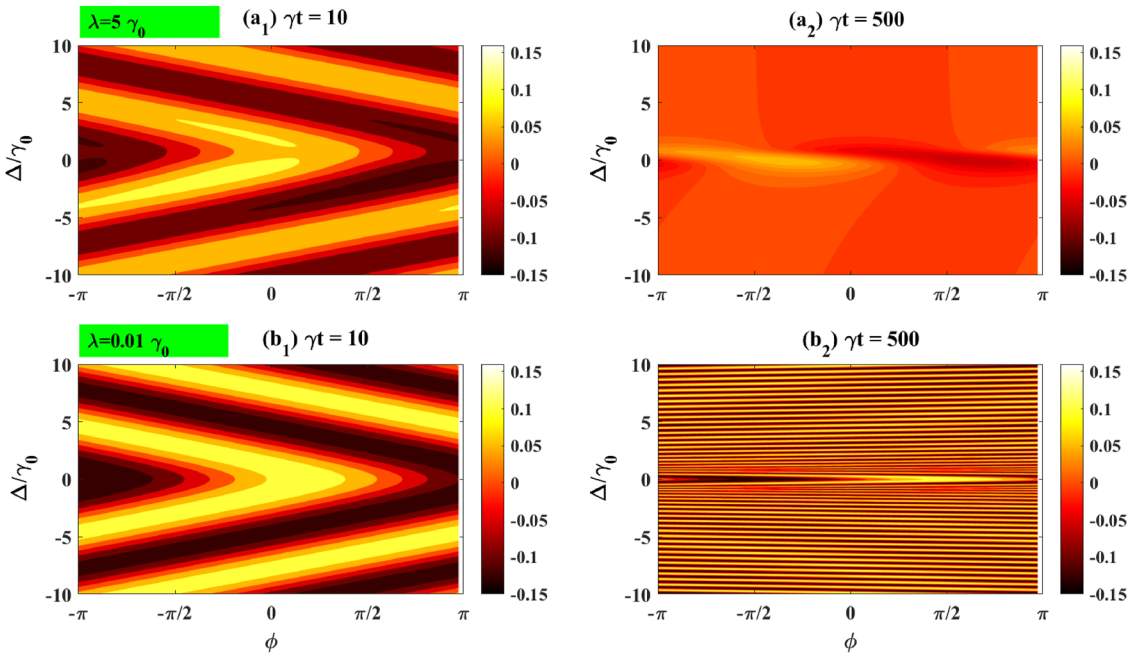

FIG. 3. Contour plot of the phase shift distribution $S(\phi,t)$ as a function of Δ and ϕ for different evolution times $\gamma_0 t$ is shown with (a) $\epsilon = 1$ in Markov case with broad reservoir spectrum ($\lambda = 5\gamma_0$) and (b) $\epsilon = 1$ in non-Markovian case with narrow spectral density ($\lambda = 0.01\gamma_0$). The system–environment coupling strength is taken as $\gamma = 0.1\gamma_0$.

localization is present even in the long-time limit for a structured reservoir with a narrow frequency spectrum.

B. Arnold tongue

Another measure that is widely used to characterize quantum synchronization is the maximum of the shifted phase distribution. This value can be found by computing $S(\phi, t)$ over the entire range of ϕ and finding the maximal value. For the single qubit system that we are investigating, the expression for the maximal shifted phase distribution $S_m(t)$ reads

$$\max\ S(\phi, t) \equiv S_m(t) = \frac{1}{4}|\rho_{10}| = \frac{1}{8}C_{\ell_1}(\rho), \tag{18}$$

where $C_{\ell_1}(\rho)$ is the ℓ_1-norm measure of quantum coherence. This connection between quantum phase localization and quantum coherence was discussed in detail in Ref. 43. This is deemed to be a natural connection because the relative phases which are being localized are the same ones that describe the quantum coherence in the system.

A contour plot of $S_m(t)$ as a function of the detuning parameter Δ and laser driving strength ϵ is shown in Fig. 4 for the reservoir in the Markovian regime, characterized by a broad frequency spectrum and negligible memory, as well as for the non-Markovian regime, where the reservoir is structured with a narrow frequency spectrum. The Markovian regime with a wide spectrum ($\lambda = 5\gamma_0$) is shown through the plots in Fig. 4(a) where $S_m(t)$ is given for $\gamma t = 10$ in Fig. 4(a1) and for $\gamma t = 500$ in Fig. 4(a2), respectively. From the plots, we observe certain regions near $\Delta \approx 0$ where $S_m(t)$ is positive, indicating that there is a region where the phases are localized. The evolution of $S_m(t)$ corresponding to the non-Markovian regime ($\lambda = 0.01\gamma_0$) is shown through the set of plots in Fig. 4(b), where Fig. 4(b1) provide the features for $\gamma t = 10$ and Fig. 4(b2) shows the result for $\gamma t = 500$, respectively. In Fig. 4(b1), we observe phase localization for a wider range of parameters in the short-time interval of $\gamma t = 10$. However, in the long-time ($\gamma t = 500$) shown in Fig. 4(b2), phase localization occurs only in a narrow range of the detuning Δ. We observe a triangular region where the phase is locked, a feature that is generally referred to as Arnold tongue and is considered as a signature of quantum phase synchronization.

C. Limit cycle analysis

The discussions we had so far show that the phase is localized in the driven two-level system, which we are currently investigating. In our earlier work in Ref. 43, we have shown that while phases can be localized, it does not always lead to phase synchronization. In fact, we show that the presence of Arnold tongue does not imply that there is a phase synchronization in the system. This necessitates us to find a new way to observe and analyze quantum phase synchronization. An alternative method to confirm the presence of quantum phase synchronization is through the existence of a limit cycle. In the long-time limit, if the trajectory of the driven TLS system becomes a closed trajectory, then the system is said to have a limit cycle. In our work, we have considered a single qubit and investigated it in the spin coherent basis. Here, the trajectory of the qubit

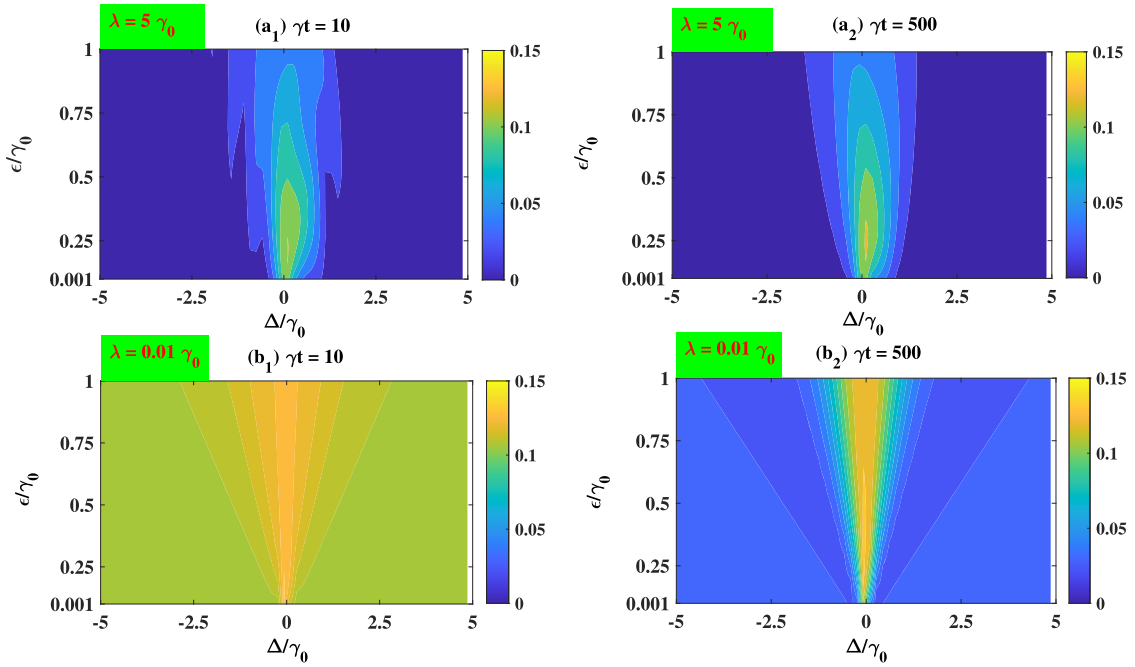

FIG. 4. Contour plot of the maximal value of the shifted phase distribution $S_m(t)$ as a function of Δ and ϵ in the Markovian regime with a wide frequency spectrum of the reservoir ($\lambda = 5\gamma_0$) for two different times (a_1) $\gamma t = 10$ and (a_2) $\gamma t = 500$. On the other hand, $S_m(t)$ as a function of Δ and ϵ is shown in the non-Markovian regime with a narrow spectrum ($\lambda = 0.01\gamma_0$) at two different times (b_1) $\gamma t = 10$ and (b_2) $\gamma t = 500$. The system–environment coupling strength is taken as $\gamma = 0.1\gamma_0$.

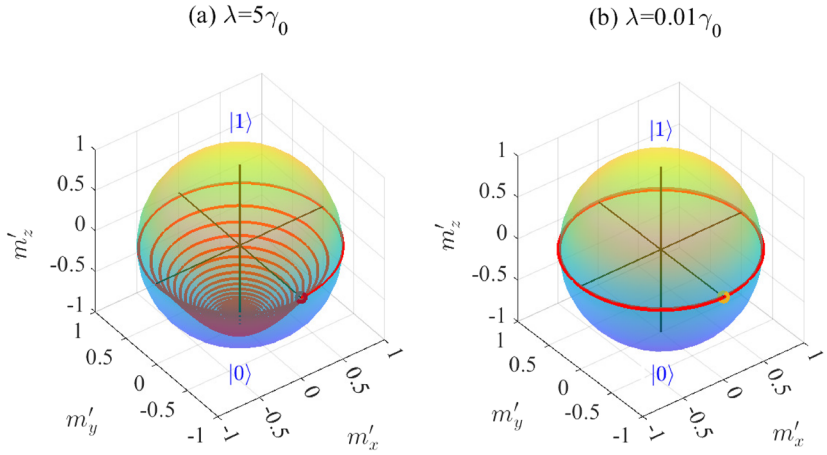

FIG. 5. Qubit trajectories on the Bloch sphere is shown for Markovian dynamics with a wide frequency spectrum of the reservoir in panel (a) with $\lambda = 5\gamma_0$ and for non-Markovian dynamics with a narrow spectrum in panel (b) with $\lambda = 0.01\gamma_0$. Values of the other parameters are taken as $\gamma = 0.1\gamma_0$, $\epsilon = \gamma_0$, and $\Delta = \gamma_0$.

in the Bloch sphere can capture its dynamics in the phase space. In the following, we present a study of the dynamics of the TLS on a three-dimensional sphere and discuss our results.

To plot the qubit trajectories on the Bloch sphere, we need to consider the system in the nonrotating frame of reference. For this, we transform the qubit density matrix with the unitary transformation $U = e^{\frac{i}{2}\sigma_z\omega_L t}$ and perform the transformation $\rho' = U^\dagger \rho U$, where ρ' is the density matrix in the nonrotating frame of reference. The Bloch vector components (m'_x, m'_y, m'_z) in the nonrotating frame can be expressed as follows:

$$m'_x = m_x \cos(\omega_L t) - m_y \sin(\omega_L t), \tag{19a}$$

$$m'_y = m_x \sin(\omega_L t) + m_y \cos(\omega_L t), \tag{19b}$$

$$m'_z = m_z, \tag{19c}$$

where $m_x = \mathrm{Tr}(\sigma_x\rho)$, $m_y = \mathrm{Tr}(\sigma_y\rho)$, and $m_z = \mathrm{Tr}(\sigma_z\rho)$ are the Bloch vector components in the rotated frame. To visualize the trajectory, we observe the dynamics of the two-level system, and for this, we plot the Bloch vector components (19a)–(19c) of the time evolved reduced density matrix of the qubit up to $\gamma_0 t = 300$ for both Markovian and non-Markovian evolution in Fig. 5. The Markovian dynamics is shown in Fig. 5(a) for $\lambda = 5\gamma_0$. We observe that the initial state $|+\rangle = (|0\rangle + |1\rangle)/\sqrt{2}$ evolves to a $|0\rangle$ state. The trajectory is not closed and the final steady state is a point on the sphere. On the contrary, the trajectory of the non-Markovian dynamics is shown in Fig. 5(b) for $\lambda = 0.01\gamma_0$, which shows that the dynamics evolves such that the trajectory is a closed curve. This feature indicates that the quantum phase of the two level system is synchronized. Thus, the limit cycle is established for the two-level system under driving and in the long-time limit the system precesses around the z axis.

V. CONCLUSION

In this work, we investigate quantum phase synchronization for a two-level system (qubit) driven by a semiclassical laser field. Two distinct types of qubit dynamics are considered depending on the reservoir correlation time being very short and a situation when bath correlation time is finite. In the Markovian regime, where the environment exhibits a broad frequency spectrum and negligible memory, the qubit's phase preference vanishes in the long-time limit. In the non-Markovian regime, characterized by a structured reservoir with narrow spectral density and finite bath correlation time, long-time phase localization persists. We used the Husimi Q-function to show that quantum phase synchronization is significantly enhanced in the non-Markovian regime. In the Markov regime with finite Δ, as the system evolves in time, the phase distribution becomes more and more uniform, and in the long-time limit, the phase preference is completely wiped out. For finite detuning, we find that the phase preference survives over a longer period in the non-Markovian dynamics in the presence of reservoir memory. To quantify the phase synchronization, we plot the shifted phase distribution and its maximum value for a wide range of system–environment parameters. The maximum of the shifted phase distribution exhibits an Arnold tongue like feature, demarcating the phase localized and phase delocalized regions in the system environment parameter space. We demonstrate a mathematical connection between the maximum of the shifted phase distribution and quantum coherence given by Eq. (18). The trajectory of the qubit in the Bloch sphere captures its dynamics in the phase space. In the long-time limit, the trajectory of the driven system becomes a closed trajectory, hence the system is said to have a limit cycle. We confirm the presence of quantum synchronization through the existence of a limit cycle. Using a shifted phase distribution $S(\phi, t)$, we show that quantum phase synchronization is significantly enhanced in the presence of reservoir memory when the spectrum is structured within a narrow frequency range. To quantify the phase synchronization, we plot the shifted phase distribution and its maximum value for a wide range of system–environment parameters. We plot the maximum of the shifted phase distribution as a function of the detuning parameter (Δ) and laser driving strength (ϵ). We systematically discussed how the synchronization regions are determined by various system–environment parameters and observed the typical Arnold tongue features of a phase synchronized qubit. Various system–environment parameters determine the synchronization regions, and the qubit phase synchronization is shown to be enhanced in the non-Markov regime. The driven qubit is synchronized inside the tongue region and desynchronized outside the

Arnold tongue. In the future, it will be interesting to investigate quantum phase synchronization under the influence of various other non-Markovian noise sources.[35–41]

ACKNOWLEDGMENTS

P.-W.C. received funding from the National Atomic Research Institute (NARI), Taiwan.

AUTHOR DECLARATIONS

Conflict of Interest

The authors have no conflicts to disclose.

Author Contributions

All the authors contributed equally to the concept, calculation, writing, and interpretation of the present work.

Po-Wen Chen: Conceptualization (equal); Data curation (equal); Formal analysis (equal); Methodology (equal); Writing – original draft (equal); Writing – review & editing (equal). **Chandrashekar Radhakrishnan**: Conceptualization (equal); Investigation (equal); Methodology (equal); Writing – original draft (equal); Writing – review & editing (equal). **Md Manirul Ali**: Conceptualization (equal); Formal analysis (equal); Investigation (equal); Methodology (equal); Writing – original draft (equal); Writing – review & editing (equal).

DATA AVAILABILITY

All data that support the findings of this study are included within the article.

REFERENCES

[1] A. Pikovsky, M. Rosenblum, and J. Kurths, *Synchronization: A Universal Concept in Nonlinear Sciences* (Cambridge University Press, UK, 2001).
[2] S. H. Strogatz, *Nonlinear Dynamics and Chaos: With Applications to Physics, Biology, Chemistry, and Engineering* (CRC Press, 2018).
[3] A. Arenas, A. Díaz-Guilera, J. Kurths, Y. Moreno, and C. Zhou, "Synchronization in complex networks," Phys. Rep. **469**, 93 (2008).
[4] B. Van der Pol, "LXXXVIII. On 'relaxation-oscillations'," London, Edinburgh Dublin Philos. Mag. J. Sci. **2**, 978 (1926).
[5] S. C. Manrubia, A. S. Mikhailov, and D. Zanette, *Emergence of Dynamical Order: Synchronization Phenomena in Complex Systems* (World Scientific, 2004), Vol. 2.
[6] G. V. Osipov, J. Kurths, and C. Zhou, *Synchronization in Oscillatory Networks* (Springer, Berlin, 2007).
[7] M. Rosenblum and A. Pikovsky, "Synchronization: From pendulum clocks to chaotic lasers and chemical oscillators," Contemp. Phys. **44**, 401 (2003).
[8] T. E. Lee and H. Sadeghpour, "Quantum synchronization of quantum van der Pol oscillators with trapped ions," Phys. Rev. Lett. **111**, 234101 (2013).
[9] S. Walter, A. Nunnenkamp, and C. Bruder, "Quantum synchronization of a driven self-sustained oscillator," Phys. Rev. Lett. **112**, 094102 (2014).
[10] N. Lörch, E. Amitai, A. Nunnenkamp, and C. Bruder, "Genuine quantum signatures in synchronization of anharmonic self-oscillators," Phys. Rev. Lett. **117**, 073601 (2016).
[11] L. Ben Arosh, M. Cross, and R. Lifshitz, "Quantum limit cycles and the Rayleigh and van der Pol oscillators," Phys. Rev. Res. **3**, 013130 (2021).
[12] O. Zhirov and D. Shepelyansky, "Synchronization and bistability of a qubit coupled to a driven dissipative oscillator," Phys. Rev. Lett. **100**, 014101 (2008).
[13] A. Roulet and C. Bruder, "Synchronizing the smallest possible system," Phys. Rev. Lett. **121**, 053601 (2018).
[14] M. Koppenhöfer and A. Roulet, "Optimal synchronization deep in the quantum regime: Resource and fundamental limit," Phys. Rev. A **99**, 043804 (2019).
[15] Á. Parra-López and J. Bergli, "Synchronization in two-level quantum systems," Phys. Rev. A **101**, 062104 (2020).
[16] X. Xiao, T.-X. Lu, W.-J. Zhong, and Y.-L. Li, "Classical-driving-assisted quantum synchronization in non-Markovian environments," Phys. Rev. A **107**, 022221 (2023).
[17] P. P. Orth, D. Roosen, W. Hofstetter, and K. Le Hur, "Dynamics, synchronization, and quantum phase transitions of two dissipative spins," Phys. Rev. B **82**, 144423 (2010).
[18] G. L. Giorgi, F. Galve, G. Manzano, P. Colet, and R. Zambrini, "Quantum correlations and mutual synchronization," Phys. Rev. A **85**, 052101 (2012).
[19] G. L. Giorgi, F. Plastina, G. Francica, and R. Zambrini, "Spontaneous synchronization and quantum correlation dynamics of open spin systems," Phys. Rev. A **88**, 042115 (2013).
[20] V. Ameri, M. Eghbali-Arani, A. Mari, A. Farace, F. Kheirandish, V. Giovannetti, and R. Fazio, "Mutual information as an order parameter for quantum synchronization," Phys. Rev. A **91**, 012301 (2015).
[21] M. R. Hush, W. Li, S. Genway, I. Lesanovsky, and A. D. Armour, "Spin correlations as a probe of quantum synchronization in trapped-ion phonon lasers," Phys. Rev. A **91**, 061401 (2015).
[22] A. Roulet and C. Bruder, "Quantum synchronization and entanglement generation," Phys. Rev. Lett. **121**, 063601 (2018).
[23] L. Henriet, "Environment-induced synchronization of two quantum oscillators," Phys. Rev. A **100**, 022119 (2019).
[24] G. Karpat, I. Yalçınkaya, and B. Çakmak, "Quantum synchronization in a collision model," Phys. Rev. A **100**, 012133 (2019).
[25] G. Karpat, I. Yalçınkaya, and B. Çakmak, "Quantum synchronization of few-body systems under collective dissipation," Phys. Rev. A **101**, 042121 (2020).
[26] I. Goychuk, J. Casado-Pascual, M. Morillo, J. Lehmann, and P. Hänggi, "Quantum stochastic synchronization," Phys. Rev. Lett. **97**, 210601 (2006).
[27] A. W. Laskar, P. Adhikary, S. Mondal, P. Katiyar, S. Vinjanampathy, and S. Ghosh, "Observation of quantum phase synchronization in spin-1 atoms," Phys. Rev. Lett. **125**, 013601 (2020).
[28] M. Koppenhöfer, C. Bruder, and A. Roulet, "Quantum synchronization on the IBM Q system," Phys. Rev. Res. **2**, 023026 (2020).
[29] L. Zhang, Z. Wang, Y. Wang, J. Zhang, Z. Wu, J. Jie, and Y. Lu, "Quantum synchronization of a single trapped-ion qubit," Phys. Rev. Res. **5**, 033209 (2023).
[30] H.-P. Breuer, E.-M. Laine, J. Piilo, and B. Vacchini, "Colloquium: Non-Markovian dynamics in open quantum systems," Rev. Mod. Phys. **88**, 021002 (2016).
[31] I. De Vega and D. Alonso, "Dynamics of non-Markovian open quantum systems," Rev. Mod. Phys. **89**, 015001 (2017).
[32] H. Eneriz, D. Rossatto, F. A. Cárdenas-López, E. Solano, and M. Sanz, "Degree of quantumness in quantum synchronization," Sci. Rep. **9**, 19933 (2019).
[33] G. Karpat, I. Yalçinkaya, B. Çakmak, G. L. Giorgi, and R. Zambrini, "Synchronization and non-Markovianity in open quantum systems," Phys. Rev. A **103**, 062217 (2021).
[34] X. Huang, Q. Ma, M. Wu, and W. Cheng, "Classical colored noise-induced quantum synchronization," Quantum Inf. Process. **22**, 431 (2023).
[35] M. M. Ali, P.-W. Chen, and H.-S. Goan, "Decoherence-free subspace and disentanglement dynamics for two qubits in a common non-Markovian squeezed reservoir," Phys. Rev. A **82**, 022103 (2010).
[36] P.-W. Chen and M. M. Ali, "Investigating Leggett–Garg inequality for a two level system under decoherence in a non-Markovian dephasing environment," Sci. Rep. **4**, 6165 (2014).
[37] C. Benedetti, F. Buscemi, P. Bordone, and M. G. Paris, "Dynamics of quantum correlations in colored-noise environments," Phys. Rev. A **87**, 052328 (2013).

[38]C. Benedetti, M. G. Paris, and S. Maniscalco, "Non-Markovianity of colored noisy channels," Phys. Rev. A **89**, 012114 (2014).
[39]M. M. Ali, P.-Y. Lo, and W.-M. Zhang, "Exact decoherence dynamics of 1/*f* noise," New J. Phys. **16**, 103010 (2014).
[40]P.-W. Chen, M. M. Ali, and S.-H. Chen, "Enhanced quantum nonlocality induced by the memory of a thermal-squeezed environment," J. Phys. A: Math. Theor. **49**, 395302 (2016).
[41]M. M. Ali and P.-W. Chen, "Probing nonclassicality under dissipation," J. Phys. A: Math. Theor. **50**, 435303 (2017).
[42]C. Radhakrishnan, P.-W. Chen, S. Jambulingam, T. Byrnes, and M. M. Ali, "Time dynamics of quantum coherence and monogamy in a non-Markovian environment," Sci. Rep. **9**, 2363 (2019).
[43]M. M. Ali, P.-W. Chen, and C. Radhakrishnan, "Detecting quantum phase localization using Arnold tongue," Physica A **633**, 129436 (2024).
[44]A. J. Leggett, S. Chakravarty, A. T. Dorsey, M. P. Fisher, A. Garg, and W. Zwerger, "Dynamics of the dissipative two-state system," Rev. Mod. Phys. **59**, 1 (1987).
[45]P. Haikka, T. Johnson, and S. Maniscalco, "Non-Markovianity of local dephasing channels and time-invariant discord," Phys. Rev. A **87**, 010103 (2013).
[46]C. Addis, G. Brebner, P. Haikka, and S. Maniscalco, "Coherence trapping and information backflow in dephasing qubits," Phys. Rev. A **89**, 024101 (2014).
[47]J. J. Burnett, A. Bengtsson, M. Scigliuzzo, D. Niepce, M. Kudra, P. Delsing, and J. Bylander, "Decoherence benchmarking of superconducting qubits," npj Quantum Inf. **5**, 54 (2019).
[48]P. Krantz, M. Kjaergaard, F. Yan, T. P. Orlando, S. Gustavsson, and W. D. Oliver, "A quantum engineer's guide to superconducting qubits," Appl. Phys. Rev. **6**, 021318 (2019).
[49]J. Etxezarreta Martinez, P. Fuentes, P. Crespo, and J. Garcia-Frias, "Time-varying quantum channel models for superconducting qubits," npj Quantum Inf. **7**, 115 (2021).
[50]K. Husimi, "Some formal properties of the density matrix," Proc. Phys.-Math. Soc. Jpn. Ser. 3 **22**, 264 (1940).
[51]R. Gilmore, C. Bowden, and L. Narducci, "Classical-quantum correspondence for multilevel systems," Phys. Rev. A **12**, 1019 (1975).